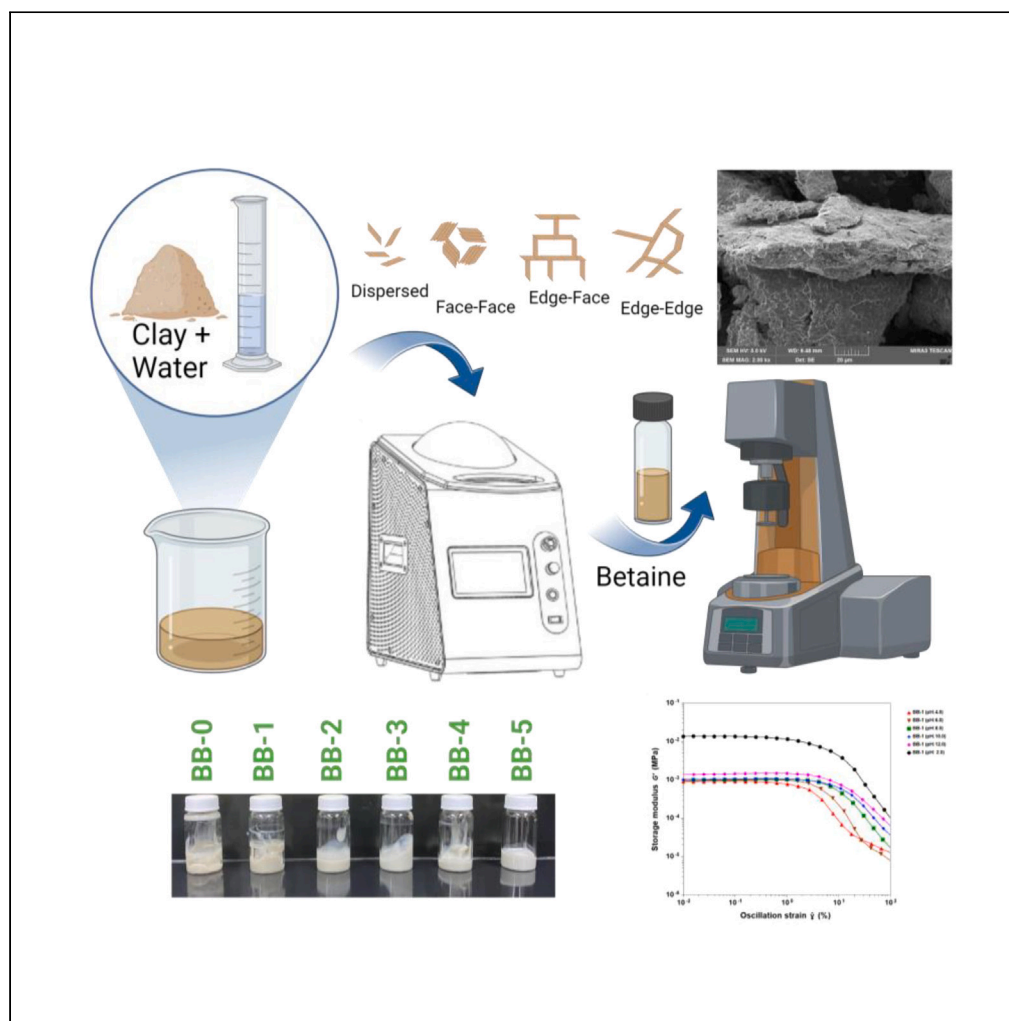


## Article

## Effect of clay-zwitterionic interactions in controlling the viscoelastic properties in organomodified clays



Pritha Sarkar,  
Suvash Ghimire,  
Sergey Vlasov,  
Kausik  
Mukhopadhyay

kausik@ucf.edu

**Highlights**

Bentonite slurries have been functionalized with betaines

Interactions between the betaines and clay on rheology have been investigated

Intercalation and rearrangement of molecules depend on betaine carbon-chain length

Clays functionalized with C1 betaine exhibited the most desirable characteristics

## Article

## Effect of clay-zwitterionic interactions in controlling the viscoelastic properties in organomodified clays

Pritha Sarkar,<sup>1,4</sup> Suvash Ghimire,<sup>1,4</sup> Sergey Vlasov,<sup>3</sup> and Kausik Mukhopadhyay<sup>1,2,5,\*</sup>

## SUMMARY

Investigating the rheology of 2D materials such as clays is of growing interest in various applications as it dictates their flowability and structural stability. Clay minerals present unique rheological properties, especially when in suspension. This study explores the effect of functionalizing bentonite clay with beta-ines of variable carbon chain lengths on the rheological properties of clay slurries to analyze their interactions in suspension. The results show that these zwitterion-functionalized clays exhibit higher viscosity, storage moduli, and flow stresses due to the formation of three-dimensional networks and increased aggregation caused by intercalation. The structural properties of the clay slurries are also found to be pH-sensitive. Additionally, XRD and SEM analyses support the proposed intercalation of the clays. The findings suggest the potential application of small-chain betaine functionalized clays in engineering and energy applications. Overall, this study provides insight into predicting the stability and strength of functionalized clay suspensions.

## INTRODUCTION

Clay minerals, essentially hydrous silicates or aluminosilicates, make up the majority of the inorganic component of soils and natural sediments and are pivotal in shaping the biogeochemistry of the earth's crust. As such, clays play a crucial role in several applications and industries.<sup>1–9</sup> Lately, they are also being used in a myriad of novel applications such as drug delivery technologies, food packaging, and battery separators.<sup>10–13</sup> The superior performance of bentonite clay is expected to drive the global market size to reach more than 3.3 billion USD with nearly 7.4% CAGR (compound annual growth rate) by 2030.<sup>14</sup> The cause driving this boom in production and innovation is that bentonite clay is a ubiquitous, inexpensive, sustainable material that can be easily functionalized for a myriad of applications.

Silica and alumina sheets form the basic structural layers of clay minerals.<sup>5,15</sup> Most clay minerals have overlapping atomic lattices with two structural units. Variations in their interactions and coordination give rise to clay minerals with roughly comparable structural similarities but distinct physical and chemical characteristics.<sup>1,4,15</sup> As a result, clay minerals have been categorized in a wide variety of ways in past literature. Generally, clay mineral structures can be broadly divided into the groups depicted in Figure 1<sup>4</sup>

Bentonite, belonging to the smectite family of clays, is classified as a 2:1 clay because it is made up of one alumina octahedral sheet sandwiched between two silica tetrahedral sheets. The apical oxygens of the tetrahedral sheets are shared by the sandwiched octahedral sheets (Figure 2).<sup>8,2</sup> In either the octahedral sheet, where  $\text{Al}^{3+}$  is replaced by charged species like  $\text{Mg}^{2+}$ ,  $\text{Fe}^{2+}$ , or  $\text{Mn}^{2+}$ , or the tetrahedral sheet, where  $\text{Si}^{4+}$  is replaced by  $\text{Al}^{3+}$  or sporadically by  $\text{Fe}^{3+}$ , the layers acquire charge. Each such substitution results in one negative charge for the layer.<sup>16–18</sup> The prominent basal surfaces that make up the particles' faces are the source of a substantial electric field with a negative electric potential due to this structural charge. Structure-property relationships of clays reveal that clays can be functionalized by leveraging their characteristics, making them one of the cheapest sustainable materials available.<sup>1,5,7</sup>

The swelling of the clay galleries is dependent on the nature and number of cations intercalated within. Strongly hydrated cations ( $\text{Na}^+$ ,  $\text{Li}^+$ ) can cause more swelling than less hydrated cations ( $\text{Ca}^{2+}$ ). One exceptional attribute of bentonite is the ability to swell and delaminate into single silicate layers or thin packets of layers easily in the presence of  $\text{Na}^+$  cations (CEC value of sodium bentonite clay is around 75 meq/100g).<sup>19–21</sup>

The properties of bentonite clay, including water adsorption and swelling, are similar to those of montmorillonite clay, the latter being a primary constituent of bentonite clay.<sup>22</sup> When clay particles are suspended in a solution, their stability is maintained by mutual repulsion due to the interactions between their diffuse electrical double layers when they approach each other. In clay-water systems, the double layer is

<sup>1</sup>Department of Materials Science and Engineering, University of Central Florida, Orlando, FL 32816, USA

<sup>2</sup>Advanced Materials Processing and Analysis Centre, University of Central Florida, Orlando, FL 32816, USA

<sup>3</sup>Department of Chemistry, University of Central Florida, Orlando, FL 32816, USA

<sup>4</sup>These authors contributed equally

<sup>5</sup>Lead contact

\*Correspondence: kausik@ucf.edu

<https://doi.org/10.1016/j.isci.2023.108388>



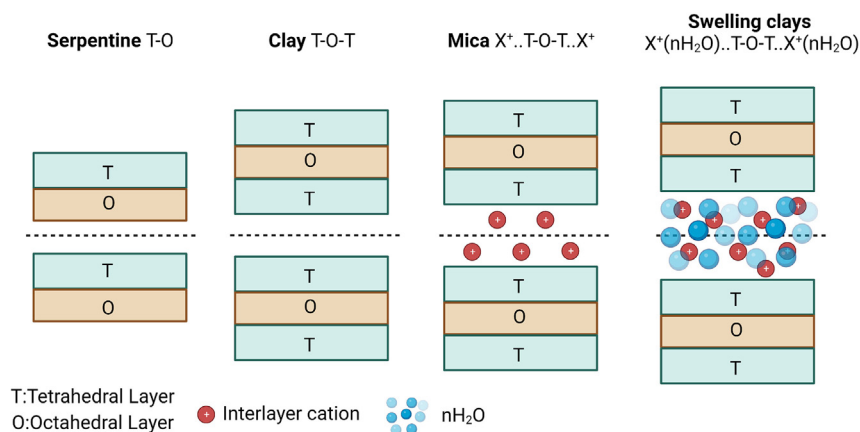


**Figure 1. Types and structures of phyllosilicate minerals**

formed by the negative surface charge and the corresponding cation charge that balances it. The negative charge of the clay particles is due to the imperfections caused within the crystal lattice. The constant surface charge of clay colloids is due to isomorphous substitution.<sup>23–25</sup> Even at relatively low concentrations, bentonite suspensions exhibit high viscosity and yield stress due to their thixotropic nature.<sup>26</sup> Bentonite can expand up to ten times its dry capacity in water and is known to form high-yield stress gels.<sup>15,27</sup> This is because the rheological characteristics are hugely influenced by the intercalation and swelling properties.<sup>28,29</sup> The rheology of clay minerals in slurries and emulsions is of developing interest since the rheology of clay slurries is highly reliant on the characteristics of the mineral particles in suspension (size, shape, surface charge, concentration, etc.).<sup>4,18,30,31</sup> The rheological behavior of clay slurries is still not well understood, nevertheless, because of their distinctive non-spherical form and anisotropic surface charge characteristics.<sup>4,15,24</sup> There is a considerable dispute in the scientific community regarding the agglomeration and flocculation properties of clay slurries.<sup>3,30,32–34</sup> Most studies support the “house-of-cards” theory for three-dimensional network structures caused by mainly three kinds of particle association—edge-face (EF), edge-edge (EE), and face-face (FF).<sup>5,35</sup> These modes are governed by several factors, such as clay concentration, electric double-layer interactions, and pH of the medium.<sup>5,36,37</sup>

Numerous studies have focused on altering clay using organic molecules for diverse applications, such as the treatment of wastewater and the adsorption of organic pollutants like pesticides, herbicides, and pharmaceuticals.<sup>6,38</sup> The rheological characteristics of organofunctionalized clay slurries are influenced by various factors, including the nature and concentration of organic and inorganic substituents employed, the concentration of clay in the suspension, and the nature of the clay particles themselves.<sup>4,18,39,40</sup> A new angle on functionalizing clay has been explored in this study by introducing zwitterions in the clay galleries. Betaine molecules have been widely studied due to their zwitterionic properties and non-toxic nature, and accordingly, have been adopted for this study.<sup>41–43</sup> The main goal of this study is to examine the effect of synthesized short and long (carbon) chained betaines on the rheological properties of clay slurries. Further, the influence of pH on the rheological characteristics of the functionalized clay suspensions has also been investigated. The findings of the study suggest that betaine-functionalized clay could serve as a cost-effective and simple rheological additive in products like paints, composites, cosmetics, medical products, and food-stuffs, where clay is commonly used as a rheological additive. With an appropriate selection of the carbon chain length, these betaine-functionalized clays can demonstrate superior storage moduli, thixotropic behavior, and stability compared to unfunctionalized clays.

## RESULTS AND DISCUSSION

### Powder XRD

The X-Ray diffraction (XRD) patterns of the functionalized clays are shown in Figure 3. Before this, an XPS analysis was carried out to verify the composition of the bentonite clay (Figure S7). The interlayer spacing of the functionalized clay samples can be determined by measuring the basal spacing of the 001 plane. The upward shift in the basal spacing of the clay provides strong evidence of intercalation of organic molecules or polycations into the clay galleries.<sup>44</sup> The peak observed at  $2\theta = 9.2^\circ$  is attributed to the  $d_{001}$  basal plane spacing of the clay. The d-spacing corresponding to BB-0 was calculated to be 0.96 nm, which agrees with the prior literature.<sup>44</sup> The subsequent  $d_{001}$  peak positions of the betaine-functionalized clay samples were seen to shift toward smaller angles, implying a rise in their d-spacing values. The d-spacings of the functionalized clays were found to be 1.38 nm for BB-1 and  $\sim 1.30$  nm for BB-3 and BB-5. These values are indicative of a monolayered structure resulting from betaine intercalation.<sup>45,46</sup> The other characteristic diffraction peaks observed at  $2\theta = 20.1^\circ$ ,  $26.7^\circ$ , and  $35.1^\circ$  were assigned to  $d_{111}$ ,  $d_{103}$ , and  $d_{211}$  diffraction planes of the bentonite clay, respectively.<sup>47</sup> The increased d-spacing in the functionalized clay samples suggests the successful intercalation of betaine molecules inside the clay galleries.<sup>44,47</sup> It is interesting to note the increase in the d-spacing value from BB-0 to BB-1, which does not change much after that. The effect of the betaine carbon chain length on the interplanar spacing of the clays is hence most pronounced with the initial introduction of the betaine molecules inside the galleries. Increasing the length of the betaine molecules consequently causes them to rearrange themselves in the existing space rather than expanding the galleries further, which drives the changes in rheological properties discussed in the following sections. It is important to note that some of the betaine molecules added during the functionalization

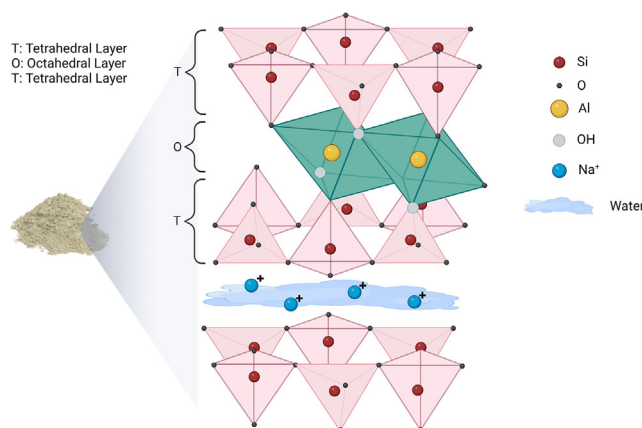


**Figure 2. Structure of bentonite clay**

process are also expected to get adsorbed on the surface of the clays. The surface areas of the functionalized clays have been calculated from BET analyses (Figure S8), which infers the functionalized samples have similar betaine surface coverages.

## Rheological analysis

### Flow sweep

Bentonite, having a 2:1 clay structure, can form hydrates with one, two, three, or four pseudo-layers of water molecules.<sup>5</sup> Water vapor, water content, and the types and concentration of salts in salt solutions all affect the state of hydration, which also depends on layer charge and interlayer cation density in salt solutions.<sup>5</sup> Figures 4A and 4B represent viscosity and shear stress values from a flow sweep test conducted on samples BB-0 through BB-5 without altering the pH of the clay slurry solution. There is noticeable significant shear thinning in all the samples as the shear rate is increased from 0.1/s to 100/s. This can be attributed to the pseudoplastic nature of the clay slurry solution.<sup>48</sup> The clay particles in the slurry suspension at rest are randomly orientated in the absence of interaction forces. Once shear is introduced, the particles begin to arrange themselves parallel to the direction of flow, which makes it easier for them to slide past one another. The individual particles thus exhibit shear-thinning flow behavior with a decrease in viscosity since they exhibit less flow resistance than in an unordered condition at rest. Further, agglomerates in the suspension imprison the dispersion liquid (water) by enclosing some of it at rest. Under shear, the superstructures gradually break down into their constituent primary particles or aggregates. The outcome is shear-thinning flow behavior with decreased viscosity at higher shear rates. The smaller superstructures exhibit less flow resistance, and the previously immobilized dispersion liquid is free to move.<sup>48</sup> There is a noticeable increase in the initial viscosity value as we move from BB-0 to BB-1, which doesn't change significantly and stabilizes thereafter, as observed from the values from BB-1 to BB-5. This may be due to a higher probability of aggregation caused by the initial intercalation of betaine molecules, which can be considered to be chemically adhered to the clay platelets. The interactions between the charged betaine molecules within the clay layers could cause increased agglomeration, resulting in higher viscosity. The FESEM micrographs show the agglomeration observed in the clay slurries post-exfoliation. As speculated, there is visible aggregation caused by the intercalation of betaine molecules. The particle sizes appear to increase in the order **BB-0** << **BB-1** ~ **BB-3** ~ **BB-5** (Figure S2).

It is also interesting to note that for BB-3 and BB-5, a brief rise in viscosity is observed around a shear rate value of 20/s before it starts dropping again. This is not seen in the plots for BB-0 and BB-1. It can be speculated that this is caused by layer distortion. Particle shape has a significant effect on flow sweep plots. The more the deviation from the original shape, the stronger this effect. This is due to the different amounts of space required by the rotating particles of different shapes and sizes. The result can be a disturbance or blockage in the flow. On intercalation, the clay galleries can be thought to be forming a monolayered structure, as inferred from the XRD analysis previously.<sup>7,49</sup> Due to the longer betaine molecules intercalated in BB-3 and BB-5 compared to BB-0 and BB-1, the zwitterionic chains are packed closer together in these layers, giving rise to more electrostatic interactions between the molecules. These interactions can be more significant at very high shear rates owing to shear around the betaine chains, resulting in more chain "entanglement". It can thus be hypothesized that betaines with chain lengths smaller than C3 do not cause significant distortion at high shear rates.

The yield stress values for betaine functionalized clays BB-1, BB-3, and BB-5 were observed to be higher than that of pure clay slurry BB-0. This shows that betaine intercalation affects the dimensional stability and structural strength of the remaining clay slurries. The shear stress values flattening out at low shear suggest they have good leveling behavior and are less likely to segregate at rest.

### Amplitude sweep

The amplitude sweep oscillatory tests suggest that  $G'_{BB-5} > G'_{BB-3} > G'_{BB-1} > G'_{BB-0}$  (Figure 5A). There is, hence, a remarkable effect of betaine intercalation on the stiffness of the clay slurries; however, the effect gradually becomes less pronounced as the betaine chain length increases. This can be explained by the formation of the monolayers in the clay mentioned before. The accommodation of betaine molecules in the

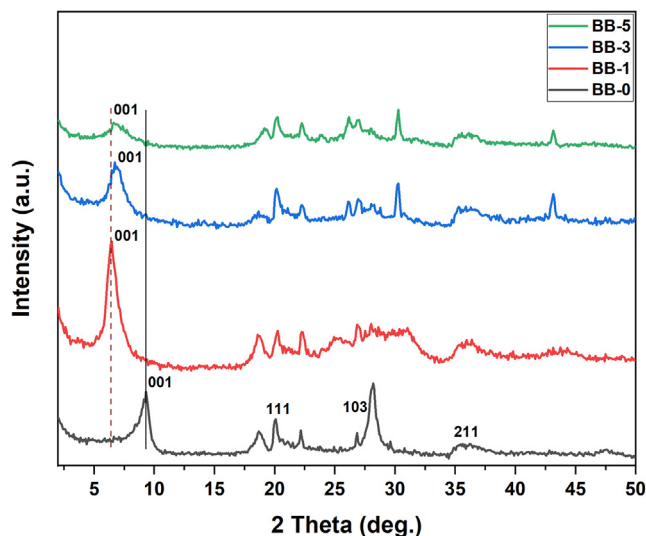


**Figure 3.** XRD spectra of BB-0, BB-1, BB-3, and BB-5, respectively

layers increases the layer spacing and introduces charge interactions in the clay galleries. These interactions increase as the betaine carbon-chain length is increased from 1C to 3C–5C. However, they maintain the monolayered structure, and the betaine chains form kinks and bend to arrange themselves in this fashion.<sup>7,49</sup> Due to this structural restriction, the rise in the stiffness reaches saturation. The observed particle sizes of the functionalized clays discussed previously also explain how the trend in agglomeration might be causing this stagnation. It should also be considered that of the betaine molecules being introduced in the clay galleries, a small fraction will be adsorbed to the surface of the clay particles. These adsorbed molecules will affect the electrical double-layer interactions in the dispersion. The existence of “train” molecules close to the surface alters the thickness of the Stern plane, which in turn alters the structure of the electrical double layer.<sup>5,50</sup> Bentonite has a very high permanent negative charge, mainly due to isomorphous substitution, where  $\text{Al}^{3+}$  in the octahedral sheet is replaced by  $\text{Fe}^{2+}$  or  $\text{Mg}^{2+}$ , and some  $\text{Si}^{4+}$  in the tetrahedral layer is substituted by  $\text{Al}^{3+}$ . These permanent charges are mainly located on the basal face and contribute to the surface charge density of bentonite clay. This explains why montmorillonite particles tend to adsorb cations to balance the negative charge.<sup>5,50</sup> Changes in surface charge, displacement of specifically adsorbed counterions by oriented water molecules, changes in the dielectric constant, changes in the thickness of the inner layer caused by the “train” segments,<sup>51,52</sup> and changes in the outer layer caused by loops and tails all affect the repulsion term in the DLVO theory.<sup>37,53–55</sup> Although the train theory is generally applied to polymer stabilizers due to their long-chain structures, the same reasoning can be extended to long-chain betaine molecules (Figure 6).<sup>5</sup> Adsorbed layers solvated in water may significantly reduce the Hamaker constant, reducing interparticle attraction and impacting the van der Waals interaction.<sup>56</sup> Further, the linear viscoelastic region (LVR) for BB-3 and BB-5 is seen to be shorter than that for BB-1 and BB-0. This observation agrees with the speculation of layer distortion at high shear in the previous section. By the same notion, it can be deduced that for BB-3 and BB-5, at high oscillatory strain values, there is significant distortion and structural breakdown (Table 1).

It is interesting to note the peaks in the loss modulus curves before they begin dropping under high strain (Figure 5B). This is indicative of slow structural relaxation or delayed structural breakdown.<sup>31,36,57–59</sup> Overall, it can be concluded that BB-1 displays the most desirable characteristics from a structural point of view due to the modest increase in storage modulus without affecting the LVR region.

### Frequency sweep

Frequency sweep oscillatory tests were performed on the samples after determining the LVR from the amplitude sweep tests. From the data, all the clay slurry samples tested were reasonably stable (Figure 7A). Frequency-independent storage moduli is a general indicator of good stability. The higher modulus for BB-0 compared to BB-1 is somewhat counterintuitive following the results of the amplitude sweep test. This may be due to the effect of time, which is not considered during these tests. Approximately 15 min can be considered to have elapsed between the amplitude sweep test conducted and frequency sweep tests, considering factors such as instrumentation time, data handling, sample changing, etc. It has been shown in the later section that time also has an appreciable effect on the rheological properties of these samples. However, the most remarkable thing to note is the rise in moduli at low shear rates for samples BB-0 and BB-1. While the curves for BB-3 and BB-5 follow the general trend for most stable suspensions and gels, it is uncommon to see a steep rise in the moduli at low angular frequency. This indicates the formation of a continuous gel-like structure at rest in the clay slurry due to flocculation. This could be due to a gradual transformation from a face-to-face (FF) structure to an edge-to-face (EF) or edge-to-edge (EE) structure in these samples. EE and EF association have been reported to cause three-dimensional “house of cards” structures in clays that can enhance their stiffness.<sup>5</sup> While the effect of pH on clay structural changes has been studied, the effect of frequency has not been studied in much detail. Several studies have supported van Olphen’s theory on the “house of cards” structures, suggesting that the three-dimensional gel structure of bentonite clay suspensions is due to

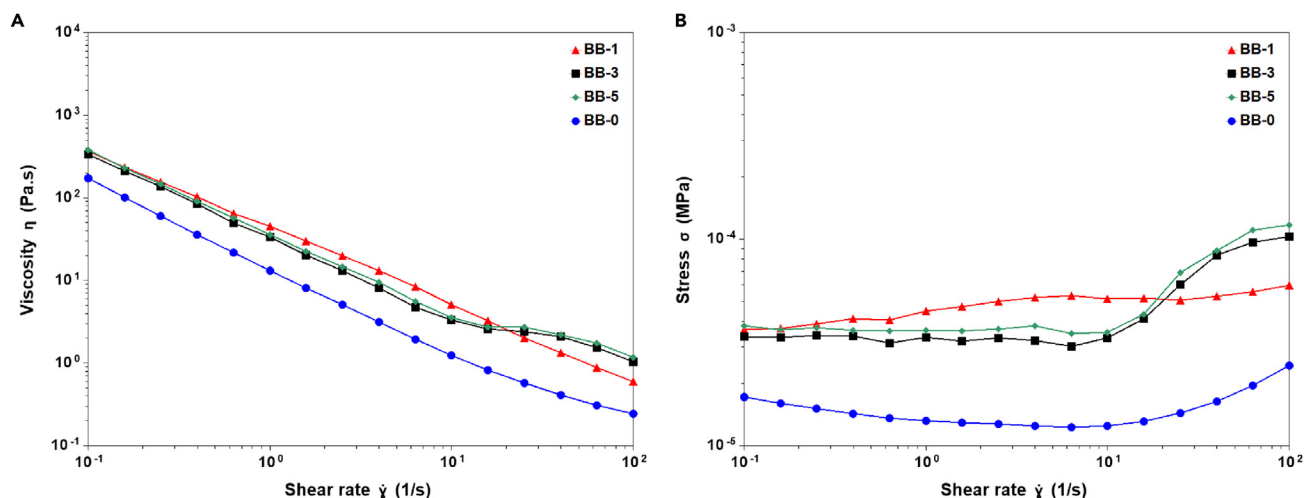


**Figure 4. Steady shear flow sweeps of functionalized clay slurries**

(A) Viscosity vs. Shear rate; (B) Shear stress vs. Shear rate.

repulsions between interacting double layers.<sup>54,60–63</sup> BB-0 and BB-1, having no and small betaine molecules in their structures, respectively, can be expected to have the strongest repulsions between their particles. At low angular frequencies mimicking long-time scales, they can form stable low-energy EF or EE configurations. Some theories suggest other stable structures, such as EE crosslinked ribbons and “Bandermodel” structures, are also possible.<sup>5</sup> Figure S3 shows that the  $\tan \delta$  values are generally around 0.1 to 0.2, characteristic of structures resistant to syneresis effects. However, BB-5 demonstrates a high  $\tan \delta$  value in the low-frequency region, which could signify phase segregation on long time-scales.<sup>53</sup> Further, a look at the surface characteristics of the samples under the SEM indicates a smooth, well-connected network for BB-0 and BB-1, unlike BB-3 and BB-5, where the morphology appears rough and disrupted. (Figures 7C–7F). This supports the inference from the frequency sweeps above regarding the formation of continuous gel-like structures at rest in the BB-0 and BB-1 slurries.

#### Time sweep and thixotropy

A time sweep test was conducted to study the stability of the clay slurries with time. When the concentration of clay reaches a certain level, flocculation can form a continuous gel structure instead of individual flocs. Over time, these gel structures slowly build up as the particles reposition themselves toward areas of minimum free energy due to Brownian motion. The concentration of clay in the system and the existence and concentration of salts present are critical factors in determining the duration required for the gel to achieve maximum strength. Typically, for  $\text{Na}^+$ -montmorillonite, this concentration is above 3% (w/w).<sup>5</sup> The clay slurries used for this study are well above this concentration. At time  $t = 0$ s, it is observed that the storage modulus of BB-3 and BB-5 are higher than those of BB-0 and BB-1, almost by a factor of 10 (Figure 8A). This agrees with the previous tests; however, a sharp increase in the moduli for BB-0 and BB-1 is seen thereafter, which is not as prominent in BB-3 and BB-5. One contributor to the increase is the loss of water while the test is running. Shear friction produces heat, leading to the evaporation of water and thickening of the matrix.<sup>64–67</sup> However, this alone does not explain the discrepancy among BB-0, BB-1, BB-3, and BB-5. This again supports the speculation that the structure is transitioning from an FF association to an EE/EF association. Further, the thixotropy loop tests agree with the betaine “train” theory discussed in the previous section. The thixotropy of clay slurries largely depends on the double-layer interactions.<sup>26,68–70</sup> When clay is sheared, the arrangement of clay particles changes to a uniform and parallel pattern. The energy applied externally breaks particle bonds, resulting in a weak and dispersed system where repulsive forces are stronger than attractive forces between particles. This process generates a slight rise in temperature, and the energy of interaction between particles remains consistent with the externally applied forces. Once the externally applied energy barrier is removed, the attractive forces overcome the repulsive forces, causing the clay-water system to adjust to a new, lower energy level. This leads to a spontaneous dissipation of excess internal energy and the formation of particle flocculation, driven by the minimum energy condition. Simultaneously, local ions in the double layer redistribute, and there is a slight alteration in the adsorbed water structure. These changes result in significant modifications to the clay’s physical behavior.<sup>26,69</sup> With enough time, the system achieves its final equilibrium, with equal attraction and repulsion forces between particles. If the double layer interactions in the clay slurry are compromised, as with the presence of the betaine “trains”, the thixotropic behavior will also be compromised, resulting in narrower thixotropic loops (Figure 8B). BB-3 and BB-5 have longer betaine molecules, demonstrating less thixotropy hysteresis than BB-0 and BB-1. BB-0, having no betaine molecules, demonstrates the most thixotropic behavior.

#### Effect of pH on the rheology of slurries

Because of the repulsive forces between their diffuse double layers, clay particles tend to stay dispersed when suspended in pure water at a low concentration. When an electrolyte, such as an acid, is present, the electrolyte ions can screen the charges on the particle surfaces,

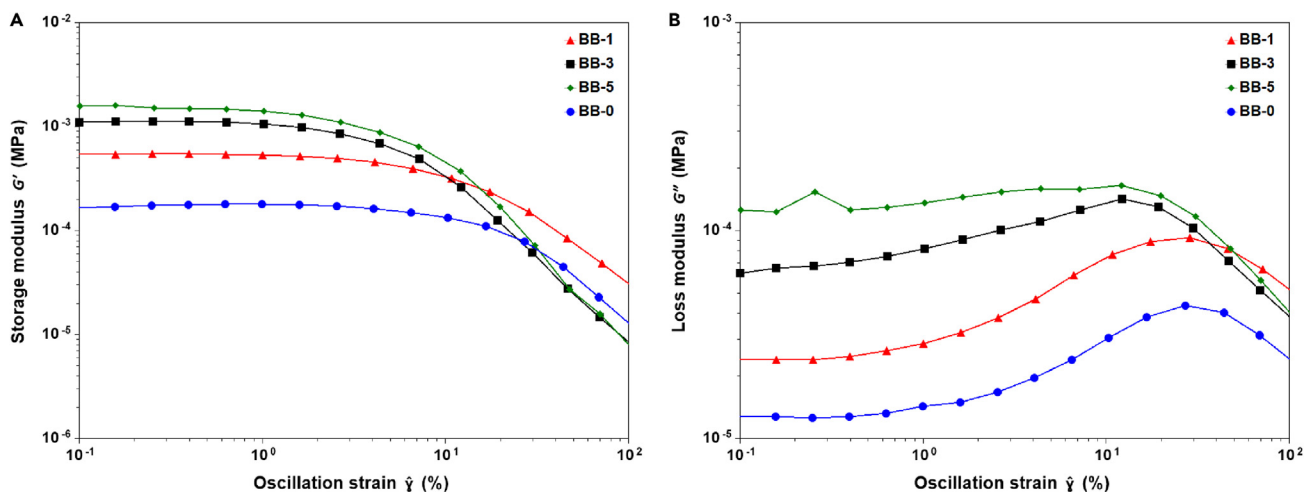


**Figure 5. Oscillatory amplitude sweeps of functionalized clay slurries**

(A) Storage moduli; (B) Loss moduli.

reducing repulsive forces and enabling the particles to move closer together. If the electrolyte concentration is raised above a critical value—the critical flocculation constant or critical coagulation concentration, the particles may come close enough to create flocs or agglomerates.<sup>40,71</sup> The valency of the cations in the electrolyte can affect the critical coagulation constant, with greater valence cations resulting in lower flocculation values.<sup>25,72</sup> This is because the more significant the charge density of the cations is, the stronger the electrostatic attraction between the particles, which can overcome the repulsive forces. The pH of the suspension can also influence how clay particles engage with one another. The surface charge of the clay varies with pH, influencing the repulsive forces that exist between them. The pH can also affect particle orientation.<sup>30,31,33,36,53,73,74</sup> As discussed earlier, the orientations and associations between the edges and faces of montmorillonite clay particles have been studied in several instances. Some researchers suggest the particles are aligned edge-to-edge (EE) in ribbons, while others believe they are aligned face-to-face (EF).<sup>5,61,63</sup> The type of association between the particles' edges and faces can be affected by the pH of the suspension. The incorporation of betaine molecules in the clay galleries can be expected to influence these interactions.

Zeta potential measurements were taken to measure the surface charges of clay particles when in suspension. It is often used to gauge the strength of the repulsive interactions between these particles.<sup>30,33</sup> Figure 9A shows that the clay-betaine slurries have a negative zeta potential over the studied pH range. This common feature of these clays implies that the clay particles carry a negative charge throughout the entire pH range. As the pH is lowered, the magnitude of the negative zeta potential decreases. This is due to the pH-dependent positive edge charges that arise and progressively neutralize the permanent negative surface charges that result from the isomorphous substitution of lower valency metal ions in the clay crystal structure.<sup>23,73–76</sup> However, even at a pH as low as 2.0, these positive edge charges are unable to neutralize the permanent negative charges,<sup>30,33,77</sup> completely. One contributing factor to this is the relatively small edge surface area, which means that the concentration of positive charges can be as low as 5% of the total surface area.<sup>30</sup> Especially in bentonite, the permanent negative charge is considerably high, constituting 90–95% of the total charges. This high negative charge density is due to the substantial degree of isomorphous substitution where  $\text{Fe}^{2+}$  or  $\text{Mg}^{2+}$  substitutes the  $\text{Al}^{3+}$  element in the octahedral sheet, and some  $\text{Al}^{3+}$  ions substitute the  $\text{Si}^{4+}$  ions in the tetrahedral layer. These permanent charges are mainly located on the basal face and account for the majority of the surface charge density of bentonite. The positive edge charges, comprising only 5–10% of the total, are insignificant in reducing this negative charge density even at extremely low pH. As a result, several studies have shown that the zeta potential of bentonite is relatively insensitive to pH changes.<sup>24,33,77</sup> However, in the presence of betaine, although still negative, there is a notable drop in the negative charge intensity at low pH. This can be attributed to the isoelectric point of betaine itself. Betaine, being a zwitterion, has its isoelectric point in the acidic regime around pH 5, below which it will be positively charged.<sup>78</sup> These positive charges, in turn, influence the net negative charge of the clay slurry. Similar reasoning has been proposed recently in a study by Shoaib et al., suggesting that different aging mechanisms and microstructural arrangements are effective in the acidic and basic regimes for clay.<sup>31</sup> This study corroborates that the strength of association increases while moving toward acidic pH from the basic regime by a concentration-pH dependency model. The rise in mean particle size observed while moving from the basic to the acidic regime suggests increased agglomeration at lower pH (Figure 9C). Zeta potential values for BB-0 and BB-1 are shown in Table S2.

The amplitude sweeps suggest that the pH of the slurry does influence aggregation in the clay particles. Although a very noticeable change is not observed as the pH of the slurry is dropped from 8.0 to 4.0 in the acidic regime, a sharp rise in the storage modulus can be seen for pH 2.0 (Figure 9B). There are two factors that can be responsible for this. As suggested previously, the increased number of positively charged species introduced due to the protonated betaine at low pH increases the number of EF associations in the suspension, resulting in increased aggregation and higher storage modulus.<sup>76,79</sup> The time sweep test supports the same trend (Figure S5). However, this alone cannot explain the sharp rise in storage modulus from pH 4.0 to 2.0. It is reasonable to assume that with the addition of HCl to lower the pH of the clay slurries, at some point between pH 4.0 and pH 2.0, the critical coagulation concentration of HCl was achieved.<sup>5,25,36</sup> It is also interesting to

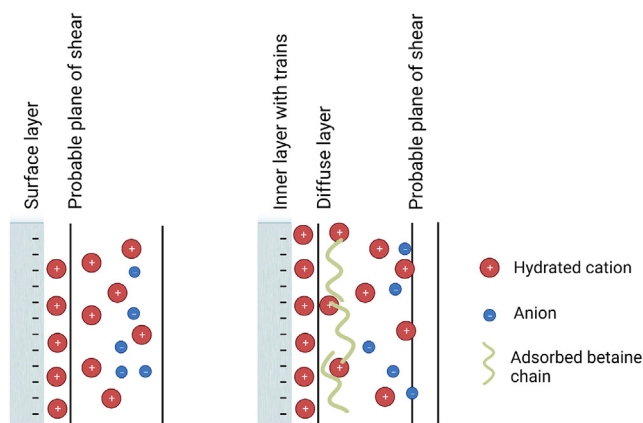


**Figure 6.** The effect of adsorbed betaine chains on the structure of the electrical double layer

note that a slight increase in the modulus is observed at pH 12. Some studies have suggested that at high pH, montmorillonite suspensions can form an open 3D network structure consisting primarily of FF-type associations that can trap more water within its layers.<sup>31,54,63</sup> This can also explain the higher storage moduli at low frequency for the slurries at high pH, as it supports the tendency of these slurries to form stable 3D networks over long timescales (Figure 9D).

## Conclusions

In the present study, bentonite clay slurries have been functionalized with betaine molecules synthesized with various carbon chain lengths, and the effect of the interactions between the betaine molecules and clay on the slurries' rheological properties has been investigated. The surface charge and rheology dependency on pH variation have also been studied. XRD and ATR-FTIR (Figure S6) confirmed the successful functionalization of the betaines in the clay by detecting new peaks post-functionalization.

Several tests were employed to comprehensively study the rheology of the functionalized clay, including flow sweep, amplitude sweep, frequency sweep, time sweep, and thixotropy. The flow sweep results showed that all the samples exhibited shear thinning behavior, indicating structural breakdown under shear. The interaction between the betaine and clay caused agglomeration, resulting in higher viscosity in functionalized clay samples. The increased storage modulus in the functionalized clay samples could also be attributed to the forming of a rigid gel-like structure and double-layer interactions. These rearrangements and interactions, in turn, brought about the rise in viscosity, storage modulus, and flow stress observed. The intercalation of betaine molecules resulted in a monolayered structure formation in the clay galleries. Increasing the chain lengths of the betaines being intercalated caused them to rearrange themselves in the existing space. The result is a significant rise in viscosity and storage moduli from BB-0 and BB-1, which gradually phases out with BB-3 and BB-5. Further, an interesting rise in storage modulus at low frequencies is observed for BB-0 and BB-1, indicative of stable network structures over long timescales. This study shows that the intercalation of longer molecules in clay galleries does not necessarily result in improved rheological performance; rather, an optimization between different rheological parameters is required. This study concludes that the BB-1 slurries functionalized with C1 betaines exhibited the most desirable characteristics due to their higher storage modulus, not sacrificing their linear viscoelastic region, and their potential to form stable connected structures. For structural applications where the significance of the storage modulus outweighs that of stability, BB-3 or BB-5 could be more favorable. It was interesting to note through this study that BB-2 slurries act somewhat differently and demonstrate a thinning effect (Figure S4). The reason behind this is currently under investigation and will be explored in future studies.

The interaction between the betaine molecules and clay platelets was sensitive to pH, as changes in pH altered the association of clay platelets, their orientations, and surface charges, which affected their rheological properties. The neutral betaine molecule becomes positively charged below its isoelectric point, which is in the acidic regime. The protonated betaine molecules at low pH led to more EF associations, increasing aggregation and higher storage modulus. However, the bentonite clay forms the open 3D network at high pH with more FF association, slightly increasing storage modulus. The sharp increase in storage modulus, flow stress, and viscosity at low pH (pH: 2.0) is due to the combined effects of protonated betaine and critical coagulation concentration of the acid being used.

Overall, using rheology, we were able to investigate the interaction between the clay and zwitterions (betaines) and how these interactions impact the structure and properties of bentonite clay. The findings provide valuable information on the effects of altering the number of carbon atoms, the chain length, and pH on the rheological properties of functionalized clays, which can benefit the scientific community and industries utilizing functionalized clays for various applications. For example, using clay as a material for battery electrodes is a significant application, typically used as a binder.<sup>80</sup> Additionally, analyzing thixotropy and the material formulation's structure recovery helps predict phase separation, precipitation, and settling, which can impact the electrode's coating and drying, subsequently affecting its quality and performance.<sup>81</sup>

Tweaking the rheological properties of clays by intercalating small, pH-sensitive, environment-friendly betaine molecules opens up new possibilities for developing clay-based functional materials. This contrasts with long-chain surfactants currently being used to make most



**Table 1. Linear Viscoelastic Region (LVR) estimation from Oscillatory amplitude sweeps**

LVR (Strain %)	
BB-0	1.6
BB-1	2.4
BB-3	4.2
BB-5	5.9

functionalized clays. The betaine-functionalized clays offer significant improvements rheologically compared to pristine, unmodified clays and are a promising alternative for non-toxic rheological additives in paints, cosmetics, and foodstuffs. By successfully functionalizing such precursors, it can also be possible to engineer sustainable clay-based sensors, devices for medical applications, and materials for energy storage and conversions in the near future.

### Limitations of the study

This study generated interesting findings that do not follow the trends of general rheology of clay materials. The higher storage moduli observed for BB-0 and BB-1 in the frequency sweep tests as opposed to the amplitude sweep tests is an example. While

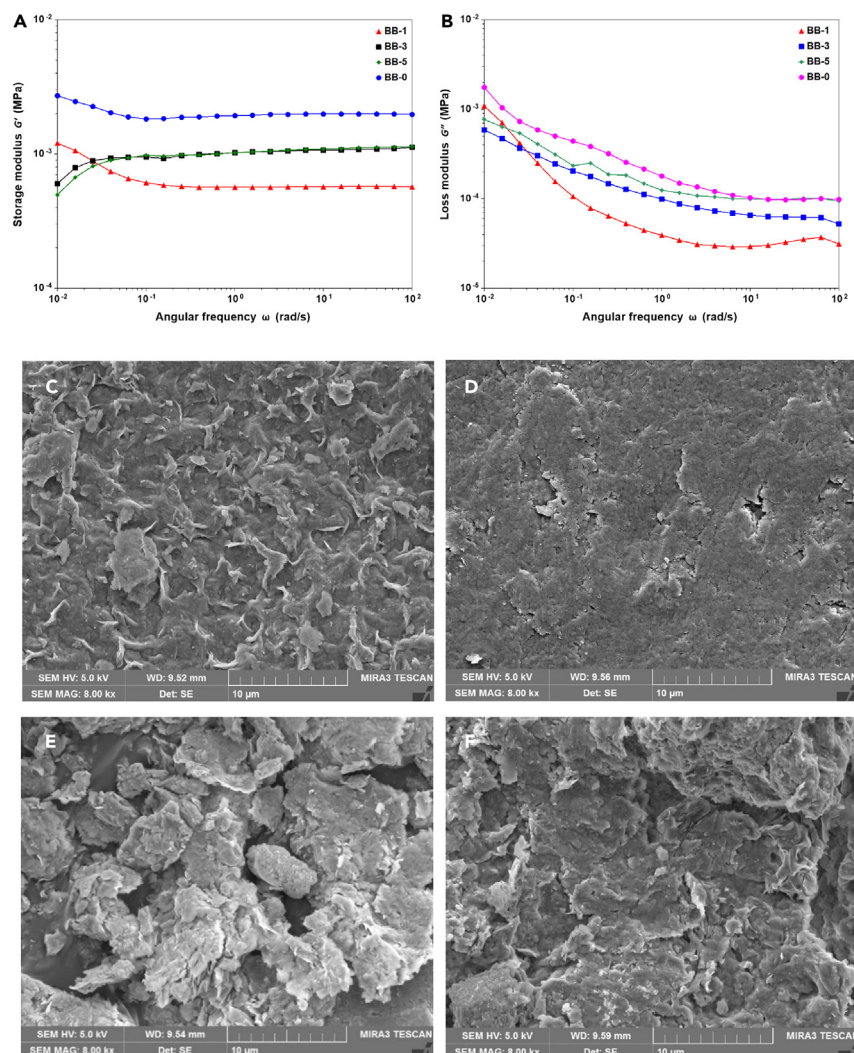


**Figure 7. Oscillatory frequency sweeps of functionalized clay slurries**

(A) Storage moduli; (B) Loss moduli; FESEM micrographs - (C) BB-0; (D) BB-1; (E) BB-3 (F) BB-5.

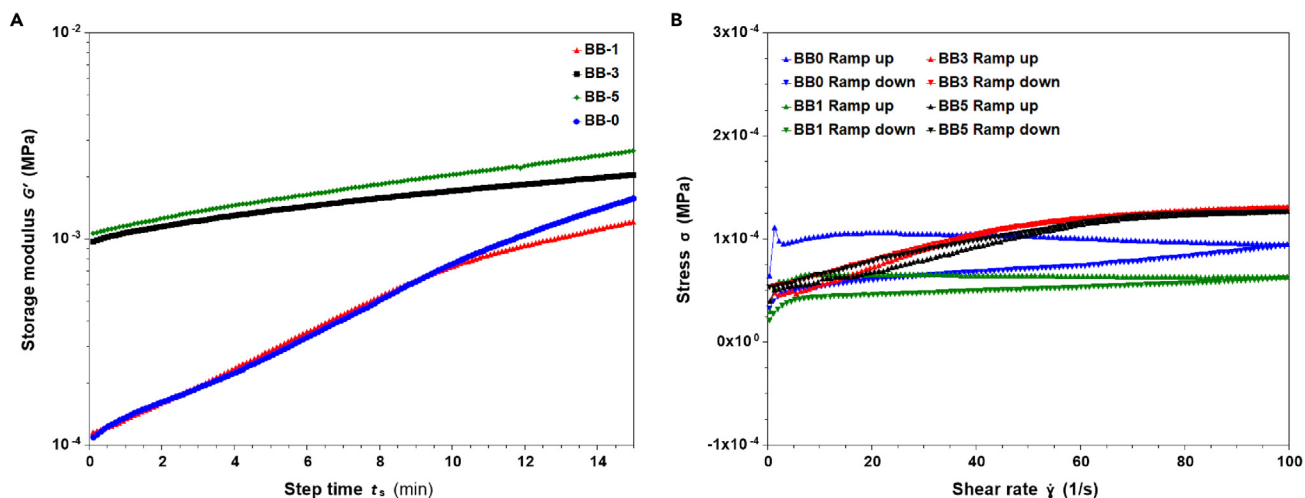


**Figure 8. Time sweeps and thixotropy hysteresis of functionalized clay slurries**  
(A) Oscillatory time sweep; (B) Oscillatory frequency ramp loop for thixotropy hysteresis.

a plausible argument has been suggested, the mechanism behind this is not entirely verifiable from these experiments. Further studies are required to dig deeper into the colloidal mechanisms of these structures. It was also intriguing to note through this study that BB-2 slurries act somewhat differently and demonstrate a thinning effect. The reason behind this is currently under investigation and will be explored in future studies.

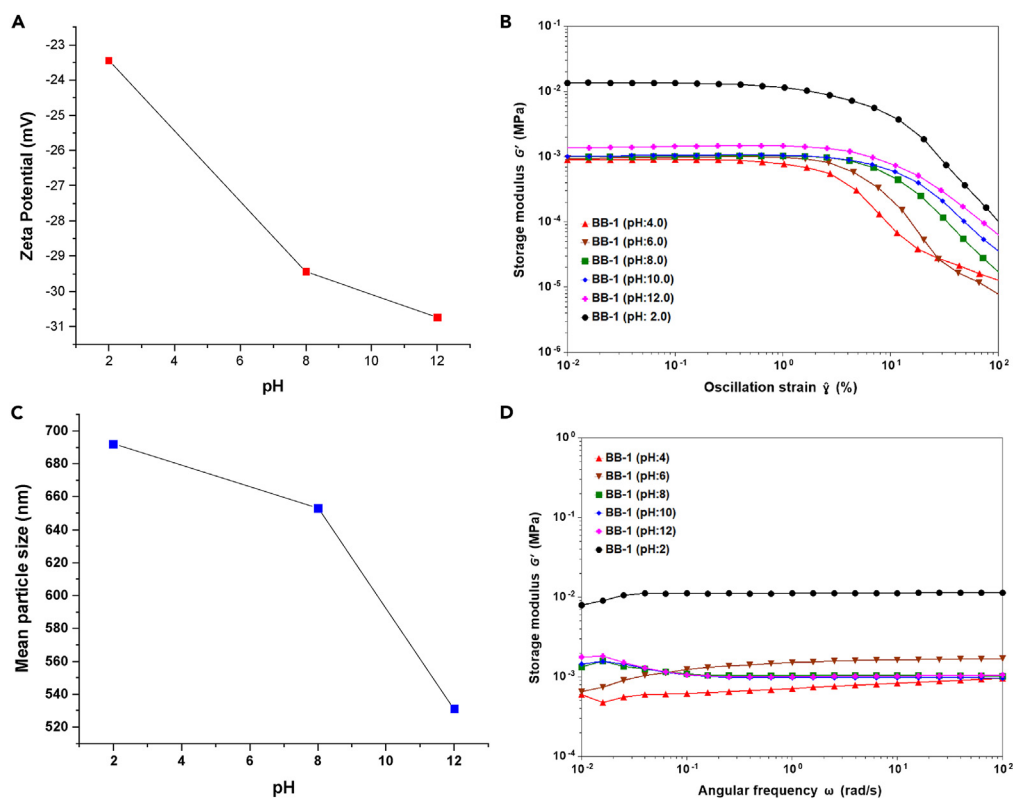


**Figure 9. Effect of pH on Betaine-functionalized clay slurries**

(A) Zeta potential vs. pH; (B) Oscillatory amplitude sweep across pH 2.0 to 12.0; (C) Particle size distribution analysis across pH 2.0 to 12.0; (D) Oscillatory frequency sweep across pH 2.0 to 12.0.

## STAR★METHODS

Detailed methods are provided in the online version of this paper and include the following:

- **KEY RESOURCES TABLE**
- **RESOURCE AVAILABILITY**
  - Lead contact
  - Materials availability
  - Data and code availability
- **METHOD DETAILS**
  - Synthesis
  - Characterization

## SUPPLEMENTAL INFORMATION

Supplemental information can be found online at <https://doi.org/10.1016/j.isci.2023.108388>.

## ACKNOWLEDGMENTS

This work was partially supported by a startup fund from UCF for Dr. K. Mukhopadhyay. We want to acknowledge the Department of Homeland Security FEMA grant for KM (grant number: EMW-2018-FP00329) for a research assistantship to support S.G.; the Trustees Doctoral Fellowship to P.S. by the UCF Board of Trustees; UCF Materials Characterization Facility (MCF) for characterization support; University of Florida, Gainesville (UF-RSC) for characterization support; Dr. Gavin Pour for help and discussions on the synthesis and characterization of the betaine molecules. We thank Dr. Sudipta Seal for allowing us to use the Tristar II Plus (Micromeritics) instrument and Yifei Fu for his assistance with the surface area analysis. All chemical structures, [Figures 1, 2, and 6](#) and the graphical abstract were made using BioRender software and created with BioRender.com. We also want to acknowledge the NSF MRI grant for XPS analyses (NSF Grant# ECCS-1726636).

## AUTHOR CONTRIBUTIONS

P.S. and S.G. made equal contributions to this work. P.S.: conceptualization, methodology, formal analysis, investigation (rheological characterization and investigation, zeta potential measurements), writing – original draft, review and editing. S.G.: conceptualization, methodology, formal analysis, investigation (sample preparation, XRD, FTIR, XPS characterization and analyses), writing – original draft, review and editing. S.V.: synthesis, formal analysis, investigation (NMR characterization, syntheses of betaines) K.M.: conceptualization, resources, writing – review and editing, supervision, project administration and management, funding acquisition.

## DECLARATION OF INTERESTS

The authors declare no competing interests.

Received: June 7, 2023

Revised: October 6, 2023

Accepted: October 31, 2023

Published: November 4, 2023

## REFERENCES

1. Bergaya, F., and Lagaly, G. (2006). Chapter 1 General Introduction: Clays, Clay Minerals, and Clay Science. *Dev Clay Sci* 1, 1–18. [https://doi.org/10.1016/S1572-4352\(05\)01001-9](https://doi.org/10.1016/S1572-4352(05)01001-9).
2. Ewis, D., Ba-Abbad, M.M., Benamor, A., and El-Naas, M.H. (2022). Adsorption of Organic Water Pollutants by Clays and Clay Minerals Composites: A Comprehensive Review. *Appl. Clay Sci.* 229, 106686. <https://doi.org/10.1016/J.CLAY.2022.106686>.
3. Kasperski, K.L., Hepler, C.T., and Hepler, L.G. (1986). Viscosities of Dilute Aqueous Suspensions of Montmorillonite and Kaolinite Clays. *Can. J. Chem.* 64, 1919–1924. <https://doi.org/10.1139/V86-316>.
4. Ndlovu, B., Becker, M., Forbes, E., Deglon, D., and Franzidis, J.P. (2011). The Influence of Phyllosilicate Mineralogy on the Rheology of Mineral Slurries. *Miner. Eng.* 24, 1314–1322. <https://doi.org/10.1016/J.Mineng.2011.05.008>.
5. Luckham, P.F., and Rossi, S. (1999). The Colloidal and Rheological Properties of Bentonite Suspensions. *Adv. Colloid Interface Sci.* 82, 43–92. [https://doi.org/10.1016/S0001-8686\(99\)00005-6](https://doi.org/10.1016/S0001-8686(99)00005-6).
6. Ghimire, S., Sarkar, P., Rigby, K., Maan, A., Mukherjee, S., Crawford, K.E., and Mukhopadhyay, K. (2021). Polymeric Materials for Hemostatic Wound Healing. *Pharmaceutics* 13, 2127. <https://doi.org/10.3390/Pharmaceutics13122127>.
7. Lagaly, G., and Beneke, K. (1991). Intercalation and Exchange Reactions of Clay Minerals and Non-Clay Layer Compounds. *Colloid Polym. Sci.* 269, 1198–1211. <https://doi.org/10.1007/BF00652529>.
8. Leporatti, S. (2019). Polymer Clay Nano-Composites. *Polymers* 11. <https://doi.org/10.3390/polym11091445>.
9. Grema, A.S., Idriss, I.M., Alkali, A.N., Ahmed, M.M., and Iyodo, M.H. (2021). Production of Clay-Based Ceramic Filter for Water Purification. *European j adv eng* 6, 140–143. <https://doi.org/10.24018/EJENG.2021.6.7.2623>.
10. Cheikh, D., Majdoub, H., and Darder, M. (2022). An Overview of Clay-Polymer Nanocomposites Containing Bioactive Compounds for Food Packaging Applications. *Appl. Clay Sci.* 216, 106335. <https://doi.org/10.1016/J.CLAY.2021.106335>.
11. Habib, M.A., and Khoda, B. (2018). Development of Clay Based Novel Bio-Ink for 3D Bio-Printing Process. *Procedia Manuf.* 26,

- 846–856. <https://doi.org/10.1016/J.PROMFG.2018.07.105>.
12. Kim, M., Kim, J.K., Park, J.H., Kim, M., Kim, J.K., and Park, H. (2015). Clay Nanosheets in Skeletons of Controlled Phase Inversion Separators for Thermally Stable Li-Ion Batteries. *Adv. Funct. Mater.* 25, 3399–3404. <https://doi.org/10.1002/ADFM.201500758>.
  13. Jafarbeglou, M., Abdouss, M., Shoushtari, A.M., and Jafarbeglou, M. (2016). Clay Nanocomposites as Engineered Drug Delivery Systems. *RSC Adv.* 6, 50002–50016. <https://doi.org/10.1039/c6ra03942a>.
  14. Global Bentonite Market Size. Statistics Report 2030. <https://www.sphericalinsights.com/reports/bentonite-market>.
  15. Hunter, R.J. (1982). The Flow Behavior of Coagulated Colloidal Dispersions. *Adv. Colloid Interface Sci.* 17, 197–211. [https://doi.org/10.1016/0001-8686\(82\)80019-5](https://doi.org/10.1016/0001-8686(82)80019-5).
  16. Barton, C.D., and Karathanasis, A.D. (2002). *Clay Minerals. Encyclopedia Soil Sci.* 187–192.
  17. Wang, Q., Zhu, C., Yun, J., and Yang, G. (2017). Isomorphous Substitutions in Clay Materials and Adsorption of Metal Ions onto External Surfaces: A DFT Investigation. *J. Phys. Chem. C* 121, 26722–26732. <https://doi.org/10.1021/acs.jpcc.7B03488>.
  18. Pir Cakmak, F., and Keating, C.D. (2017). Combining Catalytic Microparticles with Droplets Formed by Phase Coexistence: Adsorption and Activity of Natural Clays at the Aqueous/Aqueous Interface. *Sci. Rep.* 7, 3215–3314. <https://doi.org/10.1038/s41598-017-03033-z>.
  19. Gaucher, E.C., and Blanc, P. (2006). Cement/Clay Interactions – A Review: Experiments, Natural Analogues, and Modeling. *Waste Manag.* 26, 776–788. <https://doi.org/10.1016/J.WASMAN.2006.01.027>.
  20. Kahr, G., and Madsen, F.T. (1995). Determination of the Cation Exchange Capacity and the Surface Area of Bentonite, Illite and Kaolinite by Methylene Blue Adsorption. *Appl. Clay Sci.* 9, 327–336. [https://doi.org/10.1016/0169-1317\(94\)00028-O](https://doi.org/10.1016/0169-1317(94)00028-O).
  21. Christidis, G.E. (2011). Industrial Clays. *Eur. Mineral Union Notes Mineral* 9, 341–414. <https://doi.org/10.1180/EMU-NOTES.9.9>.
  22. Salah, B.A., Gaber, M.S., Hakim, A., and Kandil, T. (2019). The Removal of Uranium and Thorium from Their Aqueous Solutions by 8-Hydroxyquinoline Immobilized Bentonite. *Minerals* 9, 626. <https://doi.org/10.3390/min9100626>.
  23. Pecini, E.M., and Avena, M.J. (2013). Measuring the Isoelectric Point of the Edges of Clay Mineral Particles: The Case of Montmorillonite. *Langmuir* 29, 14926–14934. <https://doi.org/10.1021/la403384g>.
  24. Callaghan, I.C., and Otteville, R.H. (1974). Interparticle Forces in Montmorillonite Gels. *Discuss. Faraday Soc.* 57, 110–118.
  25. Penner, D., and Lagaly, G. (2001). Influence of Anions on the Rheological Properties of Clay Mineral Dispersions. *Appl. Clay Sci.* 19, 131–142. [https://doi.org/10.1016/S0169-1317\(01\)00052-7](https://doi.org/10.1016/S0169-1317(01)00052-7).
  26. Ren, Y., Yang, S., Andersen, K.H., Yang, Q., and Wang, Y. (2021). Thixotropy of Soft Clay: A Review. *Eng. Geol.* 287, 106097. <https://doi.org/10.1016/J.Enggeo.2021.106097>.
  27. Norrish, K. (1954). The Swelling of Montmorillonite. *Discuss. Faraday Soc.* 18, 120–134.
  28. Li, J., Zhou, C., Wang, G., and Zhao, D. (2003). Study on Rheological Behavior of Polypropylene/Clay Nanocomposites. *J. Appl. Polym. Sci.* 89, 3609–3617. <https://doi.org/10.1002/app.12643>.
  29. Janek, M., and Lagaly, G. (2001). Proton Saturation and Rheological Properties of Smectite Dispersions. *Appl. Clay Sci.* 19, 121–130.
  30. Au, P.I., and Leong, Y.K. (2013). Rheological and Zeta Potential Behaviour of Kaolin and Bentonite Composite Slurries. *Colloids Surf. A Physicochem. Eng. Asp.* 436, 530–541. <https://doi.org/10.1016/J.Colsurf.2013.06.039>.
  31. Shoaib, M., Khan, S., Wani, O.B., Abdala, A., Seiphooori, A., and Bobicki, E.R. (2022). Modulation of Soft Glassy Dynamics in Aqueous Suspensions of an Anisotropic Charged Swelling Clay through PH Adjustment. *J. Colloid Interface Sci.* 606, 860–872. <https://doi.org/10.1016/J.JCIS.2021.08.034>.
  32. Lagaly, G. (1989). Principles of Flow of Kaolin and Bentonite Dispersions. *Appl. Clay Sci.* 4, 105–123. [https://doi.org/10.1016/0169-1317\(89\)90003-3](https://doi.org/10.1016/0169-1317(89)90003-3).
  33. Saka, E.E., and Güler, C. (2006). The Effects of Electrolyte Concentration, Ion Species and PH on the Zeta Potential and Electrokinetic Charge Density of Montmorillonite. *Clay Miner.* 41, 853–861. <https://doi.org/10.1180/0009855064140224>.
  34. Melton, I.E., and Rand, B. (1977). Particle Interactions in Aqueous Kaolinite Suspensions: II. Comparison of Some Laboratory and Commercial Kaolinite Samples. *J. Colloid Interface Sci.* 60, 321–330. [https://doi.org/10.1016/0021-9797\(77\)90291-0](https://doi.org/10.1016/0021-9797(77)90291-0).
  35. Duc, M., Gaboriaud, F., and Thomas, F. (2005). Sensitivity of the Acid–Base Properties of Clays to the Methods of Preparation and Measurement: 1. Literature Review. *J. Colloid Interface Sci.* 289, 139–147. <https://doi.org/10.1016/J.JCIS.2005.03.060>.
  36. Shoaib, M., Cruz, N., and Bobicki, E.R. (2022). Effect of PH-Modifiers on the Rheological Behaviour of Clay Slurries: Difference between a Swelling and Non-Swelling Clay. *Colloids Surf. A Physicochem. Eng. Asp.* 643, 128699. <https://doi.org/10.1016/J.COLSURFA.2022.128699>.
  37. Tombácz, E., Nyilas, T., Libor, Z., and Csanaki, C. (2004). Surface Charge Heterogeneity and Aggregation of Clay Lamellae in Aqueous Suspensions. *Prog. Colloid Polym. Sci.* 125, 206–215. [https://doi.org/10.1007/978-3-540-45119-8\\_35](https://doi.org/10.1007/978-3-540-45119-8_35).
  38. Venancio, L.P.R., Silva, M.I.A., da Silva, T.L., Moschetta, V.A.G., de Campos Zuccari, D.A.P., Almeida, E.A., and Bonini-Domingos, C.R. (2013). Pollution-Induced Metabolic Responses in Hypoxia-Tolerant Freshwater Turtles. *Ecotoxicol. Environ. Saf.* 97, 1–9. <https://doi.org/10.1016/J.ECOENV.2013.06.035>.
  39. Blachier, C., Jacquet, A., Mosquet, M., Michot, L., and Baravian, C. (2014). Impact of Clay Mineral Particle Morphology on the Rheological Properties of Dispersions: A Combined X-Ray Scattering, Transmission Electronic Microscopy and Flow Rheology Study. *Appl. Clay Sci.* 87, 87–96. <https://doi.org/10.1016/j.clay.2013.11.004>.
  40. Du, M., Liu, J., Clode, P., and Leong, Y.K. (2019). Microstructure and Rheology of Bentonite Slurries Containing Multiple-Charge Phosphate-Based Additives. *Appl. Clay Sci.* 169, 120–128. <https://doi.org/10.1016/J.CLAY.2018.12.023>.
  41. Arumugam, M.K., Paal, M.C., Donohue, T.M., Ganesan, M., Osna, N.A., and Kharbanda, K.K. (2021). Beneficial Effects of Betaine: A Comprehensive Review. *Biology* 10, 456. <https://doi.org/10.3390/BIOLOGY10060456>.
  42. Kelleppan, V.T., King, J.P., Butler, C.S.G., Williams, A.P., Tuck, K.L., and Tabor, R.F. (2021). Heads or Tails? The Synthesis, Self-Assembly, Properties and Uses of Betaine and Betaine-like Surfactants. *Adv. Colloid Interface Sci.* 297, 102528. <https://doi.org/10.1016/J.CIS.2021.102528>.
  43. Machado, V.G., Stock, R.I., and Reichardt, C. (2014). Pyridinium N-phenolate betaine dyes. *Chem. Rev.* 114, 10429–10475. <https://doi.org/10.1021/CR5001157>.
  44. Jung, Y., Son, Y.H., Lee, J.K., Phuoc, T.X., Soong, Y., and Chyu, M.K. (2011). Rheological Behavior of Clay-Nanoparticle Hybrid-Added Bentonite Suspensions: Specific Role of Hybrid Additives on the Gelation of Clay-Based Fluids. *ACS Appl. Mater. Interfaces* 3, 3515–3522. <https://doi.org/10.1021/am200742b>.
  45. Perelomov, L., Mandzhieva, S., Minkina, T., Atroshchenko, Y., Perelomova, I., Bauer, T., Pinsky, D., and Barakhov, A. (2021). The Synthesis of Organoclays Based on Clay Minerals with Different Structural Expansion Capacities. *Minerals* 11, 707. 2021. <https://doi.org/10.3390/MIN11070707>.
  46. Lagaly, G. (1986). INTERACTION OF ALKYLAMINES WITH DIFFERENT TYPES OF LAYERED COMPOUNDS. *Solid State Ionics* 22, 43–51.
  47. Zhang, H., Kim, Y.K., Hunter, T.N., Brown, A.P., Lee, J.W., and Harbottle, D. (2017). Organically Modified Clay with Potassium Copper Hexacyanoferrate for Enhanced Cs+ Adsorption Capacity and Selective Recovery by Flotation. *J. Mater. Chem. A Mater.* 5, 15130–15143. <https://doi.org/10.1039/c7ta03873a>.
  48. Mezger, T. (2018). *Applied Rheology - with Joe Flow on Rheology Road*, 2nd ed. (Anton Paar GmbH).
  49. Lagaly, G., Ogawa, M., and Dékány, I. (2013). Clay Mineral–Organic Interactions. *Dev. Clay Sci.* 5, 435–505. <https://doi.org/10.1016/B978-0-08-098258-8.00015-8>.
  50. Murray, H.H. (1991). Overview — Clay Mineral Applications. *Appl. Clay Sci.* 5, 379–395. [https://doi.org/10.1016/0169-1317\(91\)90014-Z](https://doi.org/10.1016/0169-1317(91)90014-Z).
  51. Dunn, A.S. (1986). Polymeric Stabilization of Colloidal Dispersions. *Polym. Int.* 18, 278. <https://doi.org/10.1002/PL.4980180420>.
  52. Dickinson, E., and Eriksson, L. (1991). Particle Flocculation by Adsorbing Polymers. *Adv. Colloid Interface Sci.* 34, 1–29. [https://doi.org/10.1016/0001-8686\(91\)80045-L](https://doi.org/10.1016/0001-8686(91)80045-L).
  53. Comer, J.E.A. (2007). Ionization Constants and Ionization Profiles 5, 357–397. <https://doi.org/10.1016/B978-0-12-409547-2.11233-8>.
  54. van Olphen, H. (1964). Internal Mutual Flocculation in Clay Suspensions. *J. Colloid Sci.* 19, 313–322. [https://doi.org/10.1016/0095-8522\(64\)90033-9](https://doi.org/10.1016/0095-8522(64)90033-9).
  55. Bhattacharjee, S., Ko, C.H., and Elimelech, M. (1998). DLVO Interaction between Rough Surfaces. *Langmuir* 14, 3365–3375. <https://doi.org/10.1021/LA971360B>.
  56. Hamaker, H.C. (1937). The London—van Der Waals Attraction between Spherical Particles. *Physica* 4, 1058–1072. [https://doi.org/10.1016/S0031-8914\(37\)80203-7](https://doi.org/10.1016/S0031-8914(37)80203-7).
  57. Hyun, K., Kim, S.H., Ahn, K.H., and Lee, S.J. (2002). Large Amplitude Oscillatory Shear as a Way to Classify the Complex Fluids.

- J. Nonnewton. *Fluid Mech.* 107, 51–65. [https://doi.org/10.1016/S0377-0257\(02\)00141-6](https://doi.org/10.1016/S0377-0257(02)00141-6).
58. Miyazaki, K., Wyss, H.M., Weitz, D.A., Reichman, D.R., Xin, F.-L., Bai, X.-X., and Qian, L.-J. (2006). Nonlinear Viscoelasticity of Metastable Complex Fluids. *Europhys. Lett.* 75, 915–921. <https://doi.org/10.1209/EPL/I2006-10203-9>.
  59. Wyss, H.M., Miyazaki, K., Mattsson, J., Hu, Z., Reichman, D.R., and Weitz, D.A. (2007). Strain-Rate Frequency Superposition: A Rheological Probe of Structural Relaxation in Soft Materials. *Phys. Rev. Lett.* 98, 238303. <https://doi.org/10.1103/PHYSREVLETT.98.238303>.
  60. Ottewill, R.H. (1977). Stability and Instability in Disperse Systems. *J. Colloid Interface Sci.* 58, 357–373. [https://doi.org/10.1016/0021-9797\(77\)90148-5](https://doi.org/10.1016/0021-9797(77)90148-5).
  61. Dijkstra, M., Hansen, J.P., and Madden, P.A. (1995). Gelation of a Clay Colloid Suspension. *Phys. Rev. Lett.* 75, 2236–2239. <https://doi.org/10.1103/PhysRevLett.75.2236>.
  62. Shalkevich, A., Stradner, A., Bhat, S.K., Muller, F., and Schurtenberger, P. (2007). Cluster, Glass, and Gel Formation and Viscoelastic Phase Separation in Aqueous Clay Suspensions. *Langmuir* 23, 3570–3580. <https://doi.org/10.1021/la062996i>.
  63. van Olphen, H., M'Ewen, M.B., and Pratt, M.I. (1958). The Gelation of Montmorillonite. *Trans. Faraday Soc.* 54, 144–145. <https://doi.org/10.1039/TF9585400144>.
  64. Moller, P., Fall, A., Chikkadi, V., Derks, D., and Bonn, D. (2009). An Attempt to Categorize Yield Stress Fluid Behaviour. *Philos Trans Royal Soc A* 367, 5139–5155. <https://doi.org/10.1098/RSTA.2009.0194>.
  65. Cipolletti, L., and Ramos, L. (2005). Slow Dynamics in Glassy Soft Matter. *J. Condens Matter Phys* 17, R253–R285. <https://doi.org/10.1088/0953-8984/17/6/R01>.
  66. Joshi, Y.M. (2014). Dynamics of Colloidal Glasses and Gels. *Annu. Rev. Chem. Biomol. Eng.* 5, 181–202. <https://doi.org/10.1146/ANNUREV-CHEMBIOENG-060713-040230>.
  67. Shahin, A., and Joshi, Y.M. (2012). Physicochemical Effects in Aging Aqueous Laponite Suspensions. *Langmuir* 28, 15674–15686. <https://doi.org/10.1021/LA302544Y>.
  68. Mitchell, J.K. (1960). Fundamental Aspects of Thixotropy in Soils. *J. Soil Mech. Found Div.* 86, 19–52. <https://doi.org/10.1061/JSFEAQ.0000271>.
  69. Zhang, X.W., Kong, L.W., Yang, A.W., and Sayem, H.M. (2017). Thixotropic Mechanism of Clay: A Microstructural Investigation. *Soils Found.* 57, 23–35. <https://doi.org/10.1016/J.SANDEF.2017.01.002>.
  70. Mewis, J., and Wagner, N.J. (2011). Thixotropy. *Colloidal Suspension Rheology*, 228–251. <https://doi.org/10.1017/CBO9780511977978.010>.
  71. Ganley, W.J., and Van Duijneveldt, J.S. (2015). Controlling Clusters of Colloidal Platelets: Effects of Edge and Face Surface Chemistries on the Behavior of Montmorillonite Suspensions. *Langmuir* 31, 4377–4385. <https://doi.org/10.1021/ACS.LANGMUIR.5B00047>.
  72. Viani, B.E., Low, P.F., and Roth, C.B. (1983). Direct Measurement of the Relation between Interlayer Force and Interlayer Distance in the Swelling of Montmorillonite. *J. Colloid Interface Sci.* 96, 229–244. [https://doi.org/10.1016/0021-9797\(83\)90025-5](https://doi.org/10.1016/0021-9797(83)90025-5).
  73. Delhorme, M., Labbez, C., Caillet, C., and Thomas, F. (2010). Acid-Base Properties of 2:1 Clays. I. Modeling the Role of Electrostatics. *Langmuir* 26, 9240–9249. <https://doi.org/10.1021/la100069g>.
  74. Tombácz, E., and Szekeres, M. (2004). Colloidal Behavior of Aqueous Montmorillonite Suspensions: The Specific Role of PH in the Presence of Indifferent Electrolytes. *Appl. Clay Sci.* 27, 75–94. <https://doi.org/10.1016/J.CLAY.2004.01.001>.
  75. Sposito, G., Skipper, N.T., Sutton, R., Park, S., Soper, A.K., and Greathouse, J.A. (1999). Surface Geochemistry of the Clay Minerals. *Proc. Natl. Acad. Sci. USA* 96, 3358–3364. <https://doi.org/10.1073/PNAS.96.7.3358>.
  76. Benna, M., Kbir-Arighuib, N., Magnin, A., and Bergaya, F. (1999). Effect of PH on Rheological Properties of Purified Sodium Bentonite Suspensions. *J. Colloid Interface Sci.* 218, 442–455. <https://doi.org/10.1006/JCIS.1999.6420>.
  77. Goh, R., Leong, Y.-K., Lehane, B., Goh, R., Leong, Y.-K., and Lehane, B. (2011). Bentonite Slurries-Zeta Potential, Yield Stress, Adsorbed Additive and Time-Dependent Behaviour. *Rheol. Acta* 50, 29–38. <https://doi.org/10.1007/s00397-010-0498-x>.
  78. Lochhead, R.Y. (2017). Basic Physical Sciences for the Formulation of Cosmetic Products. *Cosmetic Science and Technology: Theoretical Principles and Applications*, 39–76. <https://doi.org/10.1016/B978-0-12-802005-0.00003-3>.
  79. Durán, J., Ramos-Tejada, M.M., Arroyo, F.J., and González-Caballero, F. (2000). Rheological and Electrokinetic Properties of Sodium Montmorillonite Suspensions. I. Rheological Properties and Interparticle Energy of Interaction. *J. Colloid Interface Sci.* 229, 107–117. <https://doi.org/10.1006/JCIS.2000.6956>.
  80. Reynolds, C.D., Lam, J., Yang, L., and Kendrick, E. (2022). Extensional Rheology of Battery Electrode Slurries with Water-Based Binders. *Mater. Des.* 222, 111104. <https://doi.org/10.1016/J.MATDES.2022.111104>.
  81. Hawley, W.B., and Li, J. (2019). Beneficial Rheological Properties of Lithium-Ion Battery Cathode Slurries from Elevated Mixing and Coating Temperatures. *J. Energy Storage* 26, 100994. <https://doi.org/10.1016/j.est.2019.100994>.
  82. Pourhakkak, P., Taghizadeh, M., Taghizadeh, A., and Ghaedi, M. (2021). Adsorbent. *Interface Sci Technol* 33, 71–210. <https://doi.org/10.1016/B978-0-12-818805-7.00009-6>.

## STAR★METHODS

## KEY RESOURCES TABLE

REAGENT or RESOURCE	SOURCE	IDENTIFIER
Chemicals, peptides, and recombinant proteins		
Bentonite	Sigma-Aldrich (St. Louis, MO)	CAS: 1302-78-9
Conc. HCl	Fisher Scientific (Hampton, NH)	CAS: 7647-01-0
Ammonium hydroxide	Fisher Scientific (Hampton, NH)	CAS: 1336-21-6
Trimethylglycine	Fisher Scientific (Hampton, NH)	CAS: 107-43-7
Acetonitrile	Fisher Scientific (Hampton, NH)	CAS: 75-05-8
Ethanol	Fisher Scientific (Hampton, NH)	CAS: 64-17-5
Acetone	Fisher Scientific (Hampton, NH)	CAS: 67-64-1
Hexane	Fisher Scientific (Hampton, NH)	CAS: 92112-69-1
3-bromopropionic acid	TCI America (Montgomeryville, PA)	CAS: 590-92-1
4-bromobutyric acid	TCI America (Montgomeryville, PA)	CAS: 2623-87-2
5-bromovaleric acid	TCI America (Montgomeryville, PA)	CAS: 2067-33-6
6-bromohexanoic acid	TCI America (Montgomeryville, PA)	CAS: 4224-70-8
Trimethylamine	Fisher Scientific (Hampton, NH)	CAS: 75-50-3

## RESOURCE AVAILABILITY

## Lead contact

Further information and requests for resources and reagents should be directed to and will be fulfilled by the lead contact, Kausik Mukhopadhyay ([kausik@ucf.edu](mailto:kausik@ucf.edu)).

## Materials availability

Betaines were synthesized according to literature methods, as cited in the references section. This study did not generate new unique reagents.

## Data and code availability

- Data reported in this paper will be shared by the [lead contact](#) upon request.
- This paper does not report original code.
- Any additional information required to reanalyze the data reported in this paper is available from the [lead contact](#) upon request.

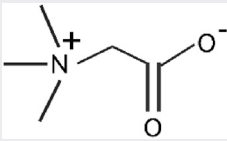
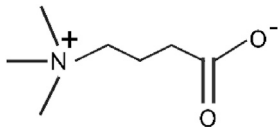
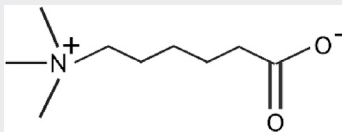
## METHOD DETAILS

## Synthesis

*Synthesis of betaines*

In this work, zwitterions, specifically variable carbon-chain betaines, were synthesized using a modified procedure following a previously reported work from literature.<sup>45</sup> In a typical synthesis, aliphatic acid bromide (1 eq) was added to a round bottom flask and dissolved in acetonitrile (1 mL/mmol of starting material). A 4.2 M solution of trimethylamine (1.5 eq) in ethanol was added to the mixture, and the solution was allowed to stir at room temperature for 12 h. This was followed by concentrating the solution under reduced pressure to approximately half its original volume and filtering. The filtered solid was rinsed with copious amounts of acetone, followed by hexane. The resultant white solid was dried under reduced pressure to obtain the betaine salt. The structures of the synthesized betaine precursors are shown in the table below and named C1, C3, and C5 betaine, where the numerals represent the number of methyl groups (-CH<sub>2</sub> groups) in the molecular structures of the betaines (Table S1 and below table). The synthesized betaines were analyzed for their structures using <sup>1</sup>H-NMR. (Figure S1). Nuclear Magnetic Resonance (NMR): <sup>1</sup>H-NMR spectra were collected using a Bruker AVANCE-III 400 MHz spectrometer. Tetramethylsilane (TMS) at 0 ppm was used as an internal standard to assign chemical shifts for <sup>1</sup>H.

### Betaine precursors and their corresponding chemical structures

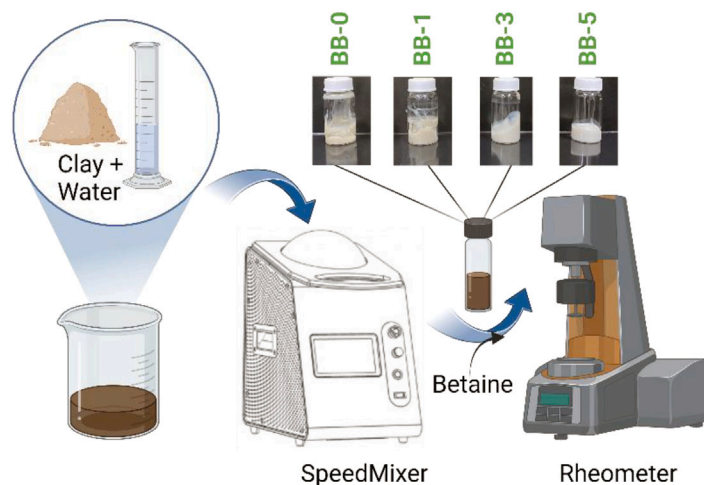
Betaine	Chemical Structure
C1 betaine <sup>a</sup>	
C3 betaine <sup>b</sup>	
C5 betaine <sup>b</sup>	

<sup>a</sup>Betaine procured from Fisher Scientific.

<sup>b</sup>Betaines synthesized in the lab.

### Betaine-functionalized clay slurries

The betaine zwitterion functionalized clay slurries were prepared by mixing 10 wt.% of bentonite clay in DI water at 2000 rpm for 60 s with a speed-mixer (Flacktek DAC330). Respective amounts of betaine were then added to the clay slurry to maintain the same number of moles across all the betaines used in this study (C1 to C5) and speed-mixed again (Clay-betaine mixing ratios are shown in table below). To allow the complete exfoliation of clay platelets and ensure proper functionalization, the slurries were agitated in a mechanical shaker (Fisherbrand™ Multi-Platform Shaker from Fisher Scientific) overnight at a speed of 300 rpm. The prepared betaine-functionalized clay slurries were then named BB-0, BB-1, BB-3, and BB-5, where BB-0 represents the unfunctionalized and BB-1, BB-3, and BB-5 represent the clay slurries functionalized with C1, C3, and C5 betaines respectively. A similar procedure was followed again to study the effect of pH on the rheological properties of the slurries. All the samples used for the pH studies were functionalized with C1 betaine. Six different samples were prepared by adjusting the pH of the slurry to 2, 4, 6, 8, 10, and 12 by dropwise addition of conc. HCl or NH<sub>4</sub>OH and the corresponding samples were named BB-1(pH:2.0); BB-1(pH:4.0); BB-1(pH:6.0); BB-1(pH:8.0); BB-1(pH:10.0); and BB-1(pH:12.0) respectively. A simplified scheme to demonstrate the slurry preparation process is shown below.



Schematic representation of clay slurry preparation.

**Clay-betaine mixing ratios**

Bentonite (wt. %)	Betaine (wt. %)	Molecular wt. of Betaine (g)	Water (wt. %)	Sample #
9	0	–	91	BB-0
9	0.4 (C1 Betaine)	117	90.6	BB-1
9	0.8 (C3 Betaine)	226	90.2	BB-3
9	0.9 (C5 Betaine)	254	90.1	BB-5

**Characterization***Zeta potential and particle size distribution*

The Malvern Zetasizer Ultra was used to measure the particle size distribution (PSD) and zeta potential of the clay slurries tested. A transfer pipette was used to collect a small amount of slurry (0.01 g) and dilute it in 0.9 ml of DI water to conduct PSD experiments. All measurements were taken in side-scatter mode at room temperature. Zeta potential measurements were made under similar conditions at a detector angle of 17°.

*Powder X-ray Diffraction (XRD)*

Powder X-ray diffraction (XRD) patterns of the betaine-functionalized clays were collected with the help of a PANalytical Empyrean X-ray diffractometer equipped with a Cu  $K_{\alpha}$  source ( $\lambda = 1.54 \text{ \AA}$ ) operated at 45 kV and 40 mA. BB-0, BB-1, BB-3, and BB-5 clay slurries were baked in a vacuum oven at 110°C for 24 h. The dry slurries were then pulverized, and the subsequent powders were analyzed. Spectra were collected over a  $2\theta$  sweep of 2° to 50° at a step size of 0.08°. Using Bragg's law, the shift in the d-spacing of the clay was analyzed to determine the intercalation of betaine molecules.

*Rheology*

A TA Instruments HR20 rheometer was used for the rheological analyses. A 25 mm stainless steel Peltier plate has been used for all experiments. All tests were in steady shear mode or oscillatory shear mode and performed at room temperature (24°C). Flow sweeps were performed in steady shear mode to measure viscosity from a shear rate of 0.01 /s to 100 /s at 5 points per decade. Amplitude sweeps were performed at an angular frequency of 10 rad/s from 0.01% strain to 100% strain. The linear viscoelastic region (LVR) was identified from the amplitude sweep to set up the frequency sweep procedure. Frequency sweeps were performed from an angular frequency of 100 rad/s to 0.01 rad/s at a fixed amplitude strain below the LVR. Time sweeps were performed at an amplitude of 1% strain and angular frequency of 10 rad/s and allowed to run for 900s. A flow sweep test to study thixotropy was set up by ramping the shear rate from 0 to 100 /s for 120 s and then ramping it back down to 0 at the same rate to produce a thixotropy loop. Data analysis was performed with the software TRIOS.

*FESEM*

The FEI Nova NanoSEM 430 was used for field emission scanning electron microscopy (FESEM). The sample slurries were baked overnight at 110°C in a vacuum oven and ground. The resulting powders were then sputtered with gold for conductivity. Micrographs were taken at an accelerating voltage of 5kV.